

A Manganese(II) Sandwich-Type Phosphotungstate Complex – Synthesis, Structural Characterization and Catalytic Activity towards Liquid-Phase Aerobic Epoxidation of Alkenes

Ketan Patel,^[a] Bharat Kumar Tripuramallu,^[b] and Anjali Patel*^[a]

Keywords: Manganese / Tungsten / Sandwich complexes / Epoxidation / Heterogeneous catalysis / Phosphotungstate

The dimeric, tetranuclear manganese(II)-substituted sandwich-type phosphotungstate complex has been synthesized in high yield using a straightforward one-pot synthesis by reacting commercially available $\text{H}_3[\text{PW}_{12}\text{O}_{40}]$ with MnCl_2 . The complex has been characterized by single-crystal X-ray

structure analysis. The complex is oxidatively and solvolytically stable and has been used as a heterogeneous catalyst in the efficient, selective aerobic epoxidation of styrene, cyclohexene and *cis*-cyclooctene.

Introduction

The enormous disparity in topology, size, electronic properties and elemental composition of polyoxometalates (POMs) provide the basis for expanding research into their chemistry.^[1] They have potential applications in areas such as catalysis, separation, sorption, ion exchange, electrochemistry, electrochromism, functional materials, magnetic and supramolecular chemistry.^[2–4] However, the mechanism for the formation of POMs is still not well understood and commonly described as self-assembly. Hence, systematic structural design of novel POMs and derivatization of known POMs remains a challenge for synthetic chemists. Among POMs, trivacant lacunary POMs are of particular interest because they present the opportunity to modify the surface properties of metal-oxide-like structural units through the replacement of several adjacent high-valent tungsten centres with low-valent transition metals.^[5] These sandwich-type POMs accommodate a number of transition metal cations between the two lacunary polyoxoanions.^[6]

Although Mn^{II} is a commonly used transition metal, tetranuclear Mn^{2+} sandwich-type POM complexes have seldom been documented. The available literature reports the synthesis of sandwich-type complexes from dilacunary^[7a] and trilacunary^[7b] POMs and from the individual salts^[7c] in complex and tedious processes. In 1993 Coronado et al. reported the synthesis and structural characterization of a Keggin-type tetranuclear sandwich complex $[\text{Mn}_4(\text{H}_2\text{O})_2(\text{PW}_9\text{O}_{34})]^{10-}$ with detailed magnetochemistry.^[7b] The reported compound was the first example of an oxo-bridged manganese cluster in +2 oxidation state with potassium counteranions.

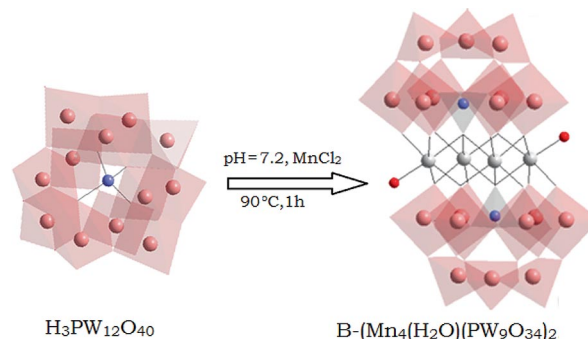
To the best of our knowledge, a one-pot synthesis for a Keggin-type tetranuclear sandwich complex $[\text{Mn}_4(\text{H}_2\text{O})_2(\text{PW}_9\text{O}_{34})]^{10-}$ has not been reported. Nevertheless, up to now catalytic epoxidation^[8] using sandwich-type phosphotungstate complexes is limited to alkenes due to complications in the synthesis of the material.

In this work, $[\text{Mn}_4(\text{H}_2\text{O})_2(\text{PW}_9\text{O}_{34})]^{10-}$ was synthesized by a straightforward one-pot route from commercially available $\text{H}_3\text{PW}_{12}\text{O}_{40}$ and MnCl_2 (Scheme 1). Our intention is to use the tailored, effective and nontoxic $[\text{Mn}_4(\text{H}_2\text{O})_2(\text{PW}_9\text{O}_{34})]^{10-}$ as a catalyst to achieve reduced costs in industry under ecologically benign conditions, with high product selectivity and reaction rates at ambient temperatures. The complex was isolated as a cesium salt and characterized by elemental analysis, thermogravimetric analysis (TGA), FTIR and ESR spectroscopy and single-crystal X-ray analysis. Furthermore, we explored the catalytic activity of the complex for liquid-phase aerobic epoxidation of alkenes.

Although Mn^{II} is a commonly used transition metal, tetranuclear Mn^{2+} sandwich-type POM complexes have seldom been documented. The available literature reports the synthesis of sandwich-type complexes from dilacunary^[7a] and trilacunary^[7b] POMs and from the individual salts^[7c] in complex and tedious processes. In 1993 Coronado et al. reported the synthesis and structural characterization of a Keggin-type tetranuclear sandwich complex $[\text{Mn}_4(\text{H}_2\text{O})_2(\text{PW}_9\text{O}_{34})]^{10-}$ with detailed magnetochemistry.^[7b] The reported compound was the first example of an oxo-bridged manganese cluster in +2 oxidation state with potassium counteranions.

To the best of our knowledge, a one-pot synthesis for a Keggin-type tetranuclear sandwich complex $[\text{Mn}_4(\text{H}_2\text{O})_2(\text{PW}_9\text{O}_{34})]^{10-}$ has not been reported. Nevertheless, up to now catalytic epoxidation^[8] using sandwich-type phosphotungstate complexes is limited to alkenes due to complications in the synthesis of the material.

In this work, $[\text{Mn}_4(\text{H}_2\text{O})_2(\text{PW}_9\text{O}_{34})]^{10-}$ was synthesized by a straightforward one-pot route from commercially available $\text{H}_3\text{PW}_{12}\text{O}_{40}$ and MnCl_2 (Scheme 1). Our intention is to use the tailored, effective and nontoxic $[\text{Mn}_4(\text{H}_2\text{O})_2(\text{PW}_9\text{O}_{34})]^{10-}$ as a catalyst to achieve reduced costs in industry under ecologically benign conditions, with high product selectivity and reaction rates at ambient temperatures. The complex was isolated as a cesium salt and characterized by elemental analysis, thermogravimetric analysis (TGA), FTIR and ESR spectroscopy and single-crystal X-ray analysis. Furthermore, we explored the catalytic activity of the complex for liquid-phase aerobic epoxidation of alkenes.



Scheme 1. Synthesis of 1.

[a] Chemistry Department, Faculty of Science, M. S. University of Baroda, Vadodara 390002, India
Fax: +91-265-2795392
E-mail: aupatel_chem@yahoo.com

[b] School of Chemistry, University of Hyderabad, Hyderabad 500046, India

Supporting information for this article is available on the WWW under <http://dx.doi.org/10.1002/ejic.201001285>.

Results and Discussion

Analytical Techniques and Crystal Structure

The observed values for the elemental analysis of the isolated complex are in good agreement with the theoretical values. The number of water molecules present was calculated from the TGA curve based on the total weight loss, and corresponds to the loss of 13 water molecules. From the elemental and thermal analyses the chemical formula is proposed to be $\text{Cs}_{10}[\text{Mn}_4(\text{H}_2\text{O})_2(\text{PW}_9\text{O}_{34})_2] \cdot 13\text{H}_2\text{O}$ (**1**). The elemental analysis for tungsten was carried out on the filtrate, and the observed percentage of W was found to be 16.56, which corresponds to the loss of three equivalents of tungsten from $\text{H}_3\text{PW}_{12}\text{O}_{40} \cdot n\text{H}_2\text{O}$.

Crystal Structure

Compound **1** crystallized in the triclinic space group $P\bar{1}$ with $a = 11.977(2)$, $b = 12.664(3)$ and $c = 16.234(3)$ Å. The crystal data are presented in Table 1.

Table 1. Crystal data and structural refinement.

Empirical formula	$\text{Cs}_{9.37}\text{Mn}_4\text{O}_{74}\text{P}_2\text{W}_{18}\text{H}_{12}$
Formula weight	6116.20
Crystal system, space group	triclinic, $P\bar{1}$
Unit cell dimensions	$a = 11.977(2)$ Å, $\alpha = 102.10(3)^\circ$ $b = 12.664(3)$ Å, $\beta = 102.69(3)^\circ$ $c = 16.234(3)$ Å, $\gamma = 105.66(3)^\circ$
Temperature	293(2) K
Volume	2216.2(8) Å ³
Z, calculated density	1, 4.583 Mg/m ³
Absorption coefficient	27.972 mm ⁻¹
$F(000)$	2616
Crystal size	0.20 × 0.16 × 0.10 mm
Theta range for data collection	1.34 to 26.41°
Limiting indices	$-14 \leq h \leq 14$ $-15 \leq k \leq 15$ $-20 \leq l \leq 20$
Reflections collected/unique	23574/8981 [$R(\text{int}) = 0.0495$]
Completeness to $\theta = 26.41$	98.9%
Absorption correction	empirical
Max./min. transmission	0.1663/0.0713
Refinement method	full-matrix least-squares on F^2
Data/restraints/parameters	8981/0/548
Goodness-of-fit on F^2	1.080
Final R indices [$I > 2\sigma(I)$]	$R_1 = 0.0467$, $wR_2 = 0.1084$
R indices (all data)	$R_1 = 0.0568$, $wR_2 = 0.1130$
Largest diff. peak and hole	3.246 and -1.875 e Å ⁻³

Single-crystal X-ray diffraction analysis shows that **1** exhibits an asymmetric dimeric structure, composed of two associated $[\alpha\text{-PW}_9\text{O}_{34}]^{9-}$ anions with four rhomb-like Mn^{2+} ions leading to a sandwich-type structure (Figure 1, left) with idealized C_{2h} point symmetry. Bond valence sum (BVS) calculations of all the manganese atoms indicate that they are all +2 valence (2.14 and 2.17 for Mn1 and Mn2, respectively).

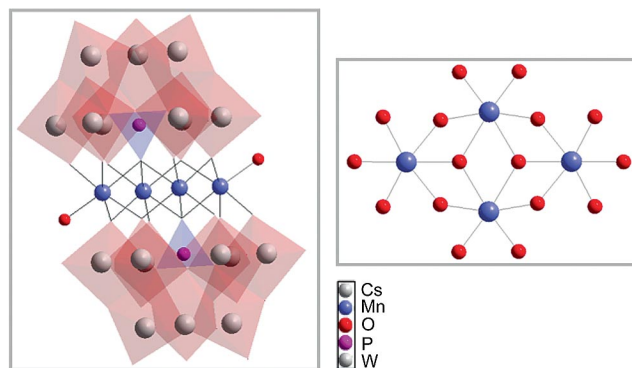


Figure 1. Left: sandwich structure of compound **1**, right: rhomb-like $\{\text{Mn}_4\text{O}_{16}\}$ unit.

BVS sum calculations for **1** indicate that the terminal oxygen atoms associated with two of the four transition metal ions (Mn^{2+}) in the central plane are the only protonation sites of the polyanion.^[9] The rhomb-like $\{\text{Mn}_4\text{O}_{16}\}$ unit (Figure 1, right) at the core of **1** contains four edge-sharing Mn^{2+} octahedra with coplanar manganese atoms, which are sandwiched by two unprecedented $[\alpha\text{-PW}_9\text{O}_{34}]^{9-}$ units. This basic building block, $[\alpha\text{-PW}_9\text{O}_{34}]^{9-}$, in **1** is similar to the well defined trivacant Keggin-type polyoxoanions, which comprise a tetrahedral PO_4 group surrounded by three edge sharing W_3O_{13} triads.

The P–O bond lengths are in the range of 1.527(11)–1.545(11) Å with an average of 1.53 Å, and the O–P–O angles range from 107.6(5) to 112.0(5)°. The O34 oxygen atom links the centrosymmetric Mn atoms to each $[\alpha\text{-PW}_9\text{O}_{34}]^{9-}$ unit with four octahedrally coordinated Mn^{2+} centres in the core. Thus, in the arrangement of the central, rhomb-like Mn_4O_{16} group the Mn^{2+} ions are all octahedrally coordinated. Two are found in the two internal positions and coordinated by two $[\alpha\text{-PW}_9\text{O}_{34}]^{9-}$ ligands, and the other two are found in the external positions and have bonding interactions with terminal water ligands in addition to the two $[\alpha\text{-PW}_9\text{O}_{34}]^{9-}$ fragments. The relevant Mn–O bond lengths are in the range of 2.082(11)–2.325(12) Å. The four Mn atoms lie at the corners of the Mn_4O_{16} unit, two opposite sides of which differ in length.

The crystal structure analysis shows that the Mn ions were not present as counteranions, and only the Cs atoms were found to be present as counteranions. The crystallographic refinement of **1** suggests the presence of 9.37 Cs atoms as counter cations, whereas the elemental analysis confirms the presence of ten Cs atoms in the formula. Based on the structural and elemental analysis, the formula of **1** is confirmed as $\text{Cs}_{10}[\text{Mn}_4(\text{H}_2\text{O})_2(\text{PW}_9\text{O}_{34})_2] \cdot 13\text{H}_2\text{O}$. The difference between the structural and elemental analyses may be due to the loss of water during single-crystal XRD data collection. The elemental composition of **1** based on X-ray diffraction is fully supported by the elemental analysis.

The powder XRD pattern of **1** is presented in Figure S1 (Supporting Information) together with the simulated pattern using the data set obtained by single crystal analy-

sis. The experimental and simulated patterns are similar indicating that the single crystal and bulk structures are identical.

Spectral Analysis

All the characteristic vibrational frequencies for **1** (Table 2) decrease compared with those of $\text{PW}_{12}\text{O}_{40}$, which is attributed to the increase of the negative charges of the anions.^[10] The characteristic vibrational modes of the PO_4 unit show that there is a loss of local symmetry as expected for the trivacant Keggin unit. The asymmetric stretching vibration of W–O–W splits into three peaks when the corresponding sandwich species are formed. In addition, the terminal W–O and bridging W–O–W stretches characteristic of all POMs are present.

Table 2. FTIR frequency data.

POMs	FTIR band frequencies [cm^{-1}]			
	P–O	W=O	W–O–W	Mn–O–W
$[\text{PW}_{12}\text{O}_{40}]^{3-}$	1080	982	893, 812	–
$[\text{Mn}_4(\text{H}_2\text{O})_2(\text{PW}_9\text{O}_{34})_2]^{10-}$	1032	940	877, 771, 740	499

A low-temperature ESR spectrum was recorded for **1** in the range of 3200–2000 G. The low temperature spectrum is well resolved showing six lines (Figure 2) with $g \approx 2.1$, which indicates the presence of Mn^{II} ions in an octahedral environment.

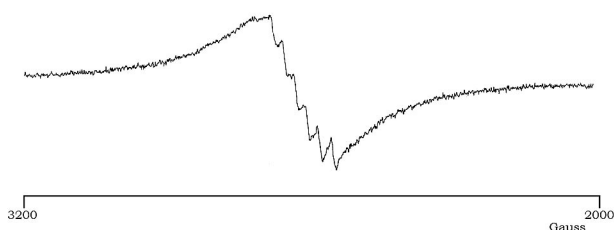


Figure 2. ESR spectrum of **1**.

Epoxidation of Alkenes

A reaction without catalyst was carried out, which showed no conversion for the substrate indicating that no auto-oxidation takes place. In order to study the role of *tert*-butyl hydroperoxide (TBHP), the same reactions were carried under two different sets of conditions: (i) alkene + oxidant + TBHP and (ii) alkene + oxidant + **1**. In both the cases the reaction did not progress significantly. These observations indicate that the liberation of O_2 from TBHP was not sufficient to induce the reaction. Hence it may be concluded that in the present study TBHP acts as an initiator only.

The O_2 -based oxidation of three representative alkenes catalyzed by **1**, and the distribution of alkene derived products obtained are reported in Table 1. It is worth noting

that, especially in case of cyclohexene, only cyclohexene oxide is obtained selectively. This unusual result may be due to the structure of the catalyst.

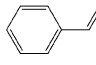
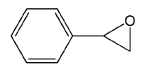
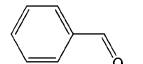
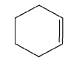
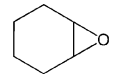

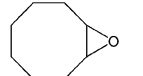
Oxidation of cyclic olefins generally follows two mechanisms: (i) oxidation and (ii) bond cleavage. In the case of cyclohexene, allylic attack (oxidation) is preferred, which results in further oxygenated products. Furthermore, it is also known that if the oxidation is carried out with an acidic catalyst using a strong oxidant with a high content of active oxygen, the bond cleavage mechanism is preferred over allylic attack resulting in the formation of cyclohexanol or cyclohexanone.^[12]

In this study, epoxidation was observed, which gave rise to cyclohexene oxide. This could be explained by the nature of the catalyst. Compound **1** is not acidic and the high electron density on the catalyst could be responsible for the stabilization of the epoxide formed.

However, it has been shown previously that decreased catalytic activity was observed when Mn^{II} is substituted into POMs.^[8a,8d] The presence of two sets of two adjacent Mn^{II} centers in our POM and their effect on the catalytic activity were therefore of interest.

Epoxidation of alkenes using $\text{H}_3\text{PW}_{12}\text{O}_{40}$ under the same conditions was carried out. In the case of styrene only 12% conversion with 98% selectivity for benzaldehyde was obtained. For cyclohexene and cyclooctene no conversion was obtained. As seen from Table 3, $\text{Cs}_5[\text{PMn}(\text{H}_2\text{O})\text{W}_{11}\text{O}_{39}] \cdot 4\text{H}_2\text{O}$ showed 61% conversion for styrene with >99% selectivity towards benzaldehyde and far less conversion for cyclohexene and cyclooctene. The difference in the catalytic activity can be explained by the structural difference between $\text{Cs}_5[\text{PMn}(\text{H}_2\text{O})\text{W}_{11}\text{O}_{39}] \cdot 4\text{H}_2\text{O}$ ^[15] and **1**. For transition metal substituted POMs, the catalytically active site is at the substituted transition metal centre, and the POM functions as a ligand with a strong capacity for accepting electrons. The incoming reactant (e.g. an alkene) directly

Table 3. Epoxidation of alkenes.

Alkenes ^[c]	Conversion (%)	Products	Selectivity (%)	TON ^[d]
	58 ^[a] /61 ^[b]		72 ^[a]	17614 ^[a] /8507 ^[b]
			28 ^[a] />99 ^[b]	
	42 ^[a] /2 ^[b]		>99 ^[a,b]	10294 ^[a] /278 ^[b]
	34 ^[a] /3 ^[b]		>99 ^[a,b]	8333 ^[a] /418 ^[b]

[a] Epoxidation of alkenes catalyzed by **1**. [b] Epoxidation of alkenes catalyzed by $\text{Cs}_5[\text{PMn}(\text{H}_2\text{O})\text{W}_{11}\text{O}_{39}] \cdot 4\text{H}_2\text{O}$. [c] Conversion based on substrate; substrate (100 mmol); oxidant: O_2 (4 mL/min); TBHP (0.15 mmol); catalyst: **1** (4.08 μmol); reaction time 4 h (for styrene) or 24 h (for cyclic olefins). [d] TON: turnover number based on conversion.

binds to the Mn^{II} centre, which is responsible for conversion. In $\text{Cs}_5[\text{PMn}(\text{H}_2\text{O})\text{W}_{11}\text{O}_{39}]\cdot 4\text{H}_2\text{O}$ only one Mn^{II} centre is present, whereas **1** has two Mn^{II} centres, which are available for binding with the incoming reactant and higher activity is observed.

Conclusions

We report here the first example of a sandwich-type complex synthesized directly from commercially available 12-phosphotungstate. This synthetic procedure opens up a new route to establish the well-known sandwich-type structures directly from their Keggin analogues. Compound **1** is an attractive heterogeneous catalyst for the epoxidation of alkenes. The superiority of the catalyst lies in its good conversion with high TON as well as selective products.

Experimental Section

Materials: All chemicals used were of A. R. grade. 12-Tungstophosphoric acid, $\text{H}_3\text{PW}_{12}\text{O}_{40}\cdot n\text{H}_2\text{O}$ (Loba Chemie, Mumbai), sodium hydroxide, $\text{MnCl}_2\cdot 4\text{H}_2\text{O}$, cesium chloride, styrene, cyclohexene, *cis*-cyclooctene and TBHP were obtained from Merck and used as received.

$[\text{Mn}_4(\text{H}_2\text{O})_2(\text{PW}_9\text{O}_{34})]^{10-}$ (1**):** $\text{H}_3\text{PW}_{12}\text{O}_{40}\cdot n\text{H}_2\text{O}$ (2.88 g) was dissolved in water (10 mL) and the pH of the solution was adjusted to 7.2 using NaOH solution (3 M). The solution was heated to 90 °C with stirring. To this hot solution, was added $\text{MnCl}_2\cdot 4\text{H}_2\text{O}$ (0.396 g) dissolved in water (10 mL). The solution was heated to 90 °C with stirring for 1 h and filtered while hot. A saturated solution of CsCl (10 mL) was added and the resulting mixture was allowed to stand overnight at room temperature. Yellow crystals of **1** were collected by filtration (yield 87.9%) and dried at 50 °C. $\text{H}_{30}\text{Cs}_{10}\text{Mn}_4\text{O}_{83}\text{P}_2\text{W}_{18}$ (6278.06): calcd. Cs 21.18, W 52.69, P 0.98, Mn 3.50, O 21.14; found Cs 20.83, W 52.38, P 0.96, Mn 3.32, O 20.58.

Characterization of **1**

Single Crystal Analysis: The single-crystal X-ray analysis was performed at 298(2) K with a Bruker SMART APEX CCD area detector system [$\lambda(\text{Mo-K}_\alpha) = 0.71973 \text{ \AA}$], graphite monochromator, 2400 frames were recorded with an ω scan width of 0.3°, each for 10 s, crystal-detector distance 60 mm, collimator 0.5 mm. The data were reduced by using SAINTPLUS and a multiscan absorption correction using SADABS^[13] was performed. Structure solution and refinement were performed using SHELX-97.^[14] All non-hydrogen atoms were refined anisotropically. During the crystallography, 39039 reflections were collected among which 8981 were unique and used to solve the structure [$R(\text{int}) = 0.0495$].

Analytical Techniques: Elemental analysis was carried out using a Prodigy high dispersion ICP (Teledyne Leeman Labs). The total weight loss was calculated by the TGA method with a Mettler Toledo Star SW 7.01 up to 600 °C. FTIR spectra of the samples were recorded as KBr pellets with a Perkin-Elmer instrument. ESR spectra were recorded with a Varian E-line Century series X-band ESR spectrometer (77 K, scanned from 2000 to 3200 Gauss). The XRD pattern was obtained using a PHILIPS PW-1830 [Cu-K_α radiation (1.54 Å)].

Epoxidation of Alkenes: The catalytic activity was evaluated for the solvent-free oxidation of alkenes using molecular oxygen as an ox-

dant and TBHP as a co-oxidant. Oxidation reactions were carried out in a batch reactor operated under atmospheric pressure. In a typical reaction, a measured amount of catalyst was added to a three-necked flask containing the alkene and TBHP (0.014 g) at 80 °C (for styrene) and 50 °C (for cyclic alkenes). The reaction was started by bubbling O_2 into the reaction medium with continuous stirring.

For the oxidation of styrene: after completion of reaction the reaction mixture was allowed to cool to room temperature and then Na_2CO_3 (10% aqueous solution) was added with constant stirring. The resultant mixture (organic and aqueous) was allowed to stand for 15–20 min in order to separate the two distinct layers. The aqueous layer was collected and concentrated aqueous HCl was added slowly with constant stirring. A white precipitate (benzoic acid) was separated and weighed (0.04 g). The remaining organic layer was washed with dichloromethane and analyzed with a gas chromatograph (Nucon 5700 model) with a flame ionization detector and an BP1 capillary column (30 m, 0.25 mm internal diameter). Product identification was carried out by comparison with authentic samples and by a combined GC–MS (Hewlett–Packard) using an HP1 capillary column (30 m, 0.5 mm internal diameter) with EI (70 eV).

For the oxidation of cyclohexene: after completion of the reaction, the neat reaction mixture was analyzed with a gas chromatograph (Nucon 5700 model) with a flame ionization detector and BP1 capillary column (30 m, 0.25 mm internal diameter), in a programmed oven (injector temperature: 200 °C, detector temperature: 250 °C, column temperature: 220 °C, ramping rate: 2.5 °C/min). No adipic acid was detected in the reaction mixture. The GC–MS spectrum of the reaction mixture was also recorded in order to confirm the absence of adipic acid. The cyclooctene oxidation product was analyzed using the same column and conditions.

The percentage-conversion of the substrate and the percentage-selectivity of the products in the epoxidation reaction are calculated as shown below.

$$\text{Conversion (\%)} = \frac{(\text{initial mol-\%}) - (\text{final mol-\%})}{\text{Initial mol-\%}} \times 100$$

$$\text{Selectivity (\%)} = \frac{\text{product formed (moles)}}{\text{Substrate converted (moles)}} \times 100$$

CCDC-422258 contains the supplementary crystallographic data for this paper. These data can be obtained free of charge from The Cambridge Crystallographic Data Centre via www.ccdc.cam.ac.uk/data_request/cif.

Supporting Information (see footnote on the first page of this article): Experimental and simulated powder XRD patterns for **1**.

Acknowledgments

K. P. is thankful to the Department of Science and Technology (DST), grant number SR/S1/IC-13/2007, New Delhi for financial support. We are thankful to UGC Networking Resource Centre, Hyderabad Central University for providing X-ray analysis facilities.

- [1] a) M. T. Pope, *Heteropoly and Isopoly Oxometalates*, Springer-Verlag, Berlin, Germany, **1983**; b) M. T. Pope, A. Muller, *Angew. Chem. Int. Ed. Engl.* **1991**, *30*, 34–48; c) C. L. Hill, *Chem. Rev.* **1998**, *98*, 1–2; for a special thematic issue, see: d) *Polyoxometalate Chemistry: From Topology via Self-Assembly to Applications* (Eds.: M. T. Pope, A. Muller), Kluwer, Dordrecht, The

- Netherlands, **2001**; e) *Polyoxometalate Chemistry for Nanocomposite Design* (Eds.: M. T. Pope, T. Yamase), Kluwer, Dordrecht, The Netherlands, **2002**; f) *Polyoxometalate Molecular Science* (Eds.: J. J. Borrás-Almenar, E. Coronado, A. Müller, M. T. Pope), Kluwer, Dordrecht, The Netherlands, **2003**.
- [2] a) *Polyoxometalates: From Platonic Solids to Anti-retroviral Activity* (Eds.: M. T. Pope, A. Müller), Kluwer, Dordrecht, The Netherlands, **1993**; b) C. L. Hill, M. Weeks, R. F. Schinazi, *J. Med. Chem.* **1990**, *33*, 2767–2772; c) J. T. Rhule, C. L. Hill, Z. Zheng, R. F. Schinazi, *Metallopharmaceuticals*, in: *Topics in Biological Inorganic Chemistry* (Eds.: M. J. Clarke, P. J. Sadler), Springer-Verlag, Heidelberg, Germany, **1999**; d) A. Seko, T. Yamase, K. J. Yamashita, *J. Inorg. Biochem.* **2009**, *103*, 1061–1066.
- [3] a) C. L. Hill, *J. Mol. Catal. A* **2007**, *262*, 2–6; b) C. L. Hill, C. M. Prosser-McCarthy, *Coord. Chem. Rev.* **1995**, *143*, 407–455; c) A. Alhanash, E. F. Kozhevnikova, I. V. Kozhevnikov, *Catal. Lett.* **2008**, *120*, 307–311; d) T. Okuhara, N. Mizuno, M. Misono, *Adv. Catal.* **1996**, *41*, 113–252; e) R. Neumann, *Prog. Inorg. Chem.* **1998**, *47*, 317–321.
- [4] D. L. Long, R. Tsunashima, L. Cronin, *Angew. Chem. Int. Ed.* **2010**, *49*, 1736–1758.
- [5] a) L. Bi, U. Kortz, B. Keita, L. Nadjo, H. Borrmann, *Inorg. Chem.* **2004**, *43*, 8367–8372; b) J. G. Liu, F. Ortega, P. Sethuraman, D. E. Katsoulis, C. E. Costello, M. T. Pope, *J. Chem. Soc., Dalton Trans.* **1992**, 1901–1906.
- [6] Y. Hou, L. Xu, M. Cichon, S. Lense, K. I. Hardcastle, C. L. Hill, *Inorg. Chem.* **2010**, *49*, 4125–4132.
- [7] a) U. Kortz, S. Isber, M. H. Dickman, D. Ravot, *Inorg. Chem.* **2000**, *39*, 2915–2922; b) C. J. Gomez Garcia, E. Coronado, P. Gomez Romero, N. Pastor, *Inorg. Chem.* **1993**, *32*, 3378–3381; c) U. Kortz, S. Nellutla, A. C. Stowe, N. S. Dalal, U. Rauwald, W. Danquah, D. Ravot, *Inorg. Chem.* **2004**, *43*, 2308–2317.
- [8] a) M. D. Ritorto, T. M. Anderson, W. A. Neiwert, C. L. Hill, *Inorg. Chem.* **2004**, *43*, 44–49; b) R. Ben-Daniel, L. Weiner, R. Neumann, *J. Am. Chem. Soc.* **2002**, *124*, 8788–8789; c) X. Zhang, T. M. Anderson, Q. Chen, C. L. Hill, *Inorg. Chem.* **2001**, *40*, 418–419; d) R. Neumann, M. Gara, *J. Am. Chem. Soc.* **1994**, *116*, 5509–5510; e) R. Neumann, M. Gara, *J. Am. Chem. Soc.* **1995**, *117*, 5066–5074.
- [9] I. D. Brown, D. Altermatt, *Acta Crystallogr., Sect. B* **1985**, *41*, 244–247.
- [10] U. Kortz, I. M. Mbomekalle, B. Keita, L. Nadjo, B. Patrick, *Inorg. Chem.* **2002**, *41*, 6412–6416.
- [11] a) L.-H. Bi, E. Wang, J. Peng, R. D. Huang, L. Xu, C. W. Hu, *Inorg. Chem.* **2000**, *39*, 671–679; b) R. Contant, R. Thouvenot, *Can. J. Chem.* **1991**, *69*, 1498–1506.
- [12] P. Shringarpure, A. Patel, *J. Mol. Chem. A* **2010**, *321*, 22–30.
- [13] *SADABS, SMART, SAINT and SHELXTL*, Bruker AXS Inc., Madison, Wisconsin, USA, **2000**.
- [14] G. M. Sheldrick, *SHELX-97, Program for Crystal Structure Solution and Analysis*, University of Göttingen, Göttingen, Germany, **1997**.
- [15] K. Patel, P. Shringarpure, A. Patel, *Trans. Met. Chem.* **2011**, *36*, 171–177.

Received: December 8, 2010
Published Online: March 9, 2011